Available online at www.sciencedirect.com
ScienceDirect
Journal of Molecular Catalysis A: Chemical 260 (2006) 227–234
JOURNAL OF MOLECULAR CATALYSIS A: CHEMICAL
www.elsevier.com/locate/molcata

Stabilization mechanism of TiO_2 on flexible fluorocarbon films as a functional photocatalyst

Yu Zhiyong [a,d], E. Mielczarski [b], J.A. Mielczarski [b], D. Laub [c], L. Kiwi-Minsker [a], A. Renken [a], J. Kiwi [a,*]

[a] *Institute of Chemical Sciences and Engineering, SB-ISIC-LGRC, Swiss Federal Institute of Technology (EPFL), Station 6, 1015 Lausanne, Switzerland*
[b] *INPL/ENG, CNRS, UMR 7569, LEM, Pole de l'Eau, 15 Av du Charmois, 54501 Vandoeuvre les-Nancy, France*
[c] *Institute of Electron Microscopy (CIME), Swiss Federal Institute of Technology (EPFL), Station 12 Lausanne 10015, Switzerland*
[d] *Department of Chemistry, Renmin University of China, Beijing 100872, China*

Received 23 May 2006; accepted 7 July 2006
Available online 24 August 2006

Abstract

The repetitive discoloration kinetics of the azo-dye Methyl Orange (taken as a model organic compound) was followed under solar simulated radiation (90 mW/cm^2) to assess the performance of the TiO_2/Tedlar® composite photocatalyst. The influence of solution parameters on the photo-discoloration process: pH, dye concentration, applied light intensity and concentration of H_2O_2 were systematically investigated. During the photocatalysis a modification occurs in the TiO_2/Tedlar® composite due to the TiO_2 interaction with the Tedlar® film. Physical insight is given for the stabilization mechanism of the TiO_2 particles in the Tedlar matrix based on the data obtained by X-ray photoelectron spectroscopy (XPS). The F 1s peak of the Tedlar film indicates that the TiO_2 is loaded on the Tedlar fluoro-groups. The loading of TiO_2 on the 75 μm thick Tedlar® film was ~0.9% (w/w) as determined by atomic absorption spectrophotometry (AAS). Attenuated total reflection infrared spectroscopy (ATRIR) shows no formation of additional bands within the photodiscoloration reaction. This shows that an efficient catalysis taking place on the TiO_2/Tedlar® surface. The rugosity (mean square roughness, rms) of the TiO_2/Tedlar® film was determined by atomic force microscopy (AFM) to be 19.7 nm. This value remained constant during long-term operation. Transmission electron microscopy (TEM) reports the thickness and coverage of TiO_2 Degussa P-25 on the Tedlar® surface before and after photocatalysis.

Keywords: Fluorocarbons films; TiO_2 stabilization; Photocatalysis; XPS; AFM; IR

1. Introduction

The use of supported photocatalysts is important since the separation of the TiO_2 after treatment in degradation processes is costly in terms of materials, labor and time. The Tedlar polymer film is the aim of this study and will be shown to have properties that allow its use as a TiO_2 support to mediate the degradation of organic compounds involving light induced redox reactions. These favourable properties are: (a) the resistance to the highly oxidative radical attack by the species formed on the TiO_2 surface, (b) the ability to preclude TiO_2 leaching during long operational periods and finally (c) the adequate process kinetics attained during repetitive degradation cycles of the model compound. Nevertheless, very little work has been carried out on TiO_2 loaded polymeric films and supports with the purpose of developing a relatively low cost decontamination photocatalyst.

Tedlar® polyvinyl fluoride (PVF) film has been selected as the inert support for this study due to its relatively low price (compared to DuPont Nafion®), high resistance to weathering, durability, mechanical resistance, chemical inertness, and good aging properties due to absence of plasticizers. TiO_2 has shown photocatalytic properties that have been widely used in the abatement and discoloration of organic dyes during the last 25 years [1,2]. Recently, our laboratory has reported the stable fixation of nanocrystalline TiO_2 on Nafion® due to the negatively charged sulfonic $-SO_3^-$ group of the Nafion film [3] interacting with the positively charged Ti^{4+} of the nanocrystalline TiO_2. The same approach was used when attaching nanocrystallyne TiO_2 to the maleic anhydride-polyethylene copolymer

* Corresponding author. Tel.: +41 21 801 7536; fax: +41 21 693 3190.
E-mail address: john.kiwi@epfl.ch (J. Kiwi).

1381-1169/$ – see front matter © 2006 Elsevier B.V. All rights reserved.
doi:10.1016/j.molcata.2006.07.021

film [4]. Several recent studies have reported the photocatalytic degradation of methylene blue on TiO_2-polstyrene [5], the abatement of porphyrins on polystyrene [6] and the use of anatase on plastic surfaces as photocatalyst [7]. A recent review reports the fixation by plasma methods of TiO_2 on polymer films [8]. The discoloration of the model azo-dye compound mediated by TiO_2 dispersions has been reported recently [9,10].

The objective of the present investigation is to report the stabilization mechanism of TiO_2 in the Tedlar perfluorocarbon matrix during the photocatalysis leading to the discoloration of a model azo-dye. The synthesis, testing and characterization with up-to-date techniques of TiO_2/Tedlar photocatalyst with a considerably lower price tag than Nafion® will be reported in this study. We have selected Methyl Orange as a model compound to test the effects of the photocatalytic performance of TiO_2/Tedlar under solar simulated irradiation since it presents suitable light absorption properties at $\lambda > 400$ nm.

2. Experimental

2.1. Materials and reagents

Methyl Orange ($NaO_3S–C_6H_4–N=N–C_6H_4–N(CH_3)_2$), acids, bases and H_2O_2 were Fluka p.a. and used as received. The TiO_2 Degussa P-25 photocatalyst was a gift from Degussa AG Switzerland, 6340 Baar. The Tedlar® A is a DuPont durable film 72 μm thick and consists of polyvinyl fluoride $(–CH_2–CHF–)_n$. The Tedlar® A film is used in the present study to bond TiO_2. The film is tough, flexible and fatigue-resistant up to 180 °C (flowing point).

2.2. Catalysts preparation

The Tedlar® A film was immersed in a solution of alcohol to which TiO_2 Degussa P-25 was subsequently added and the suspension was aged for a day. The Tedlar–TiO_2 film was then dried at room temperature and subsequently heated in an oven up to 180 °C for 10 h. Shorter times than the 10 h heating at 180 °C produced a less stable deposit of nanocrystalline-TiO_2 on the Tedlar film as seen in the course of this work. The sticking of TiO_2 to the surface is a consequence of some melting due to the treatment at 180 °C during 10 h. Finally, the TiO_2/Tedlar film was sonicated a few times in water to eliminate the loosely bound TiO_2 particles on the film.

2.3. Irradiation procedures

The photo-degradation of Methyl Orange was carried out in small batch cylindrical photochemical reactors made from Pyrex glass (cutoff $\lambda = 290$ nm) of 70 ml capacity containing 50 ml aqueous solution. The strips 48 cm^2 films of TiO_2/Tedlar were positioned immediately behind the reactor wall. Irradiation of the samples was carried out in the cavity of a Suntest solar simulator (Hanau, Germany) air cooled at 35 °C. The light flux in the cavity of the Suntest simulator at tuned at 90 mW/cm^2 (AM 1) was 2×10^{16} photons/s cm^2. The Suntest Xe-lamp emitted 7% of the photons in the 290–400 spectral range. The integral radiant flux in the reactor cavity was monitored with a powermeter from YSI Corp., CO, USA.

2.4. Analyses of the irradiated solutions

The absorption of the solutions was followed in a Hewlett-Packard 38620 N-diode array spectrophotometer. The disappearance of Methyl Orange was measured in the spectrophotometer at $\lambda = 465$ nm (the absorption peak). The peroxide concentration of the solutions were measured using Merckoquant® paper from Merck AG, Switzerland. This was carried out for reactions with initially added H_2O_2 to determine its concentration in the course of the reaction.

2.5. Transmission Electron microscopy (TEM) of TiO_2/Tedlar films

A field emission TEM microscope Philips EM 430 (300 kV) was used to measure the particle size of the titania aggregates on the textile surfaces. Energy dispersive X-ray spectroscopy (EDS) was used to identify the TiO_2 on the Tedlar film. The Tedlar film was coated with EPON 812 epoxy resin polymerized at 60 °C and then cut with a microtome at room temperature to a thin layer of about 50 nm thicknesses.

2.6. Atomic force microscopy (AFM) of TiO_2/Tedlar films

The AFM images were obtained using an AutoProbe M5 instrument of ThermoMicroscopes Inc. The intermittent contact mode and silicon cantilever with conical tip force constant was used having 13 N/m and a resonant frequency 280 kHz. All scans were performed with a set-point amplitude of 25 nm and at a scanning rate 0.5 Hz. This insured stable tip radius and no sample wear during the experiments. Images were flattened by a line-by-line (3rd order polynomial fit) using ThermoMicroscopes's image processing software. Consecutively, the roughness was calculated.

2.7. X-ray photoelectron spectroscopy (XPS) of TiO_2/Tedlar films

The X-ray photoelectron spectra were obtained with a multi-detection electron energy analyzer (VSW FAT mode CL150). The Mg radiation source (1253.6 eV) was operated at 15 kV and 10 mA. The XPS resolution between 0.1 and 0.9 eV was determined by the use of the gold standard. The operating pressure in the spectrometer was 10^{-8} mbar. Charging effects on the samples were observed. The C 1s line (284.6 eV) was used as reference to correct the sample charging effects. The recorded lines for: C 1s, F 1s, O 1s, Ti 2p, N 1s and Ca 2p were recorded in the appropriate range of binding energies in order to obtain a good signal/noise ratio. The peaks were smoothed by polynomial fit and background subtraction according to Shirley [11] and then fitted using a curve-fitting program provided with a Gaussian/Lorentzian curve generator.

2.8. Attenuated total reflection infrared Fourier transform spectroscopy (ATRIR)

This technique was applied to study the surfaces of unloaded and loaded Tedlar films. The reflection spectra were recorded on a Bruker IFS 55 FTIR spectrophotometer equipped with an MCT detector and an internal reflection attachment from Harrick Co. The Tedlar film was contacted with the ZnSe reflection element with dimensions 50 mm × 20 mm × 3 mm at an incident angle Θ of 45°. The depth of penetration (d_p) of the incident radiation, defined as the distance required for the electric field amplitude to fall to e^{-1} is calculated by the relation $D_p = \lambda_1/2\Pi(\sin^2 \Theta - n_2^2)^{1/2}$. The reflection spectra were recorded for both sides of the Tedlar film showing no difference.

3. Results and discussions

3.1. Comparison of the photo-discoloration kinetics observed with TiO_2 suspensions and TiO_2/Tedlar supported photocatalysts

The photo-discoloration of Methyl Orange by TiO_2 Degussa P-25 powders is shown in Fig. 1. The effect of the TiO_2 suspension on the discoloration of Methyl Orange in the dark and under light in the absence and presence of H_2O_2 is shown in Fig. 1. The results show that effective photocatalysis in the presence of the TiO_2 powders takes place. The addition of H_2O_2 as oxidant in this air-purged solution accelerated only slightly the rate of photodiscoloration as seen in trace (d).

Fig. 2, trace (a) shows a low degree of dye photodiscoloration at pH 5.9. But in the presence of TiO_2/Tedlar (trace (b)), the photodiscoloration readily proceed. This pH-value is simply the pH of the dye solution. The interaction between Methyl Orange and TiO_2 is favored at pH 5.9 by the positive charge of the $TiOH_2^+$ species existing on the surface of TiO_2. At a pH <7, the anion radical of Methyl Orange interacts with $TiOH_2^+$ after the Na-cation ionizes in solution [12]. Traces (c) and (d) show a lower

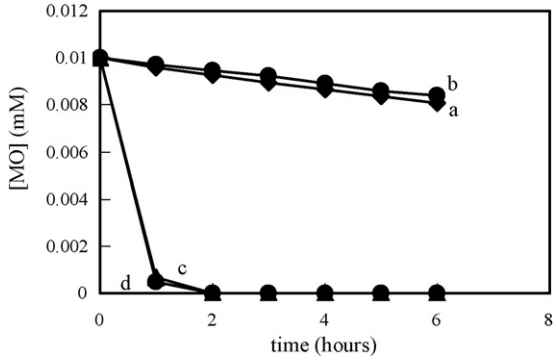

Fig. 1. Photocatalyzed degradation of Methyl Orange (0.01 mM) in a solution containing TiO_2 Degussa P-25 (0.5 g/L) at an initial pH of 5.9. (a) Dark reaction, (b) dark reaction in the presence of H_2O_2 (1 mM), (c) reaction under solar simulated light (90 mW/cm^2) and (d) reaction under solar simulated light (90 mW/cm^2) in the presence of H_2O_2 (1 mM).

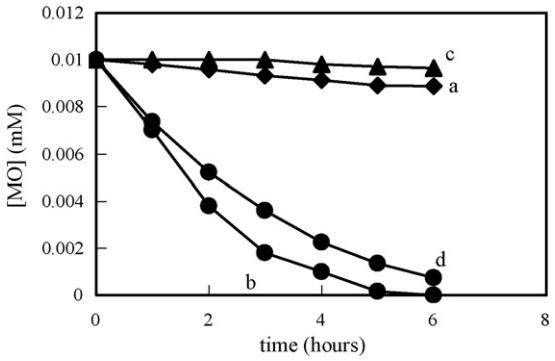

Fig. 2. Effect of the pH on the degradation of Methyl Orange (0.01 mM) under solar simulated light (90 mW/cm^2). (a) At an initial pH of 5.9, (b) at an initial pH of 5.9 in the presence of TiO_2/Tedlar photocatalyst, (c) at an initial pH of 10 and (d) at an initial pH of 10 in the presence of TiO_2/Tedlar.

discoloration of the dye possibly due to some repulsion between the TiO^- on the Tedlar surface (pH 10) and the anion radical of Mehyl Orange in solution. No discoloration was observed of Methyl Orange in solution in the dark in the presence of Tedlar alone or under light irradiation. The TiO_2/Tedlar photocatalyst was ineffective in the dark for the discoloration of Methyl Orange.

The dye molecules adsorbed on the photocatalyst surface are excited by the light photons and produce the singlet excited state, as it has been previously reported by Kamat [13] for Acid Orange 7 and by Kiwi [14] for the dye Orange II

$$(\text{Methyl Orange})_{ads} + h\nu \rightarrow {}^1(\text{Methyl Orange})_{ads}{}^* \quad (1)$$

For the family of azo-dyes, an electron can be injected from the excited state of the adsorbed of Methyl Orange on the Tedlar to the conduction band of TiO_2 leading to the formation of the Methyl Orange cation

$$ {}^1(\text{Methyl Orange})_{ads}{}^* + TiO_2 \rightarrow {}^1(\text{Methyl Orange})_{ads}{}^{\bullet+} + TiO_2\,(e^-) \quad (2)$$

and the injected electron (e^-) is subsequently scavenged by the O_2 adsorbed on the TiO_2 surface, to generate the superoxide radical $O_2^{\bullet-}$ [1–2]

$$TiO_2(e^-) + O_2 \rightarrow TiO_2 + O_2^{\bullet-} \quad (3)$$

As the pH turns to more acid values, the formation of $HO_2^\bullet$ and H_2O_2 is favored as shown by the following equations:

$$O_2^{\bullet-} + H^+ \rightarrow HO_2^\bullet \quad (4)$$

$$HO_2^\bullet + O_2^{\bullet-} + H^+ \rightarrow H_2O_2 + O_2 \quad (5)$$

$$HO_2^\bullet + H^+ + TiO_2{}^\bullet(e^-) \rightarrow H_2O_2 + TiO_2 \quad (6)$$

3.2. Effect of H_2O_2 concentration and light intensity on the photodegradation kinetics of Methyl Orange

Fig. 3 presents in traces (a) and (b) the modest photodiscoloration of a solution of Methyl Orange in the presence of two different concentrations of H_2O_2. The effect of the

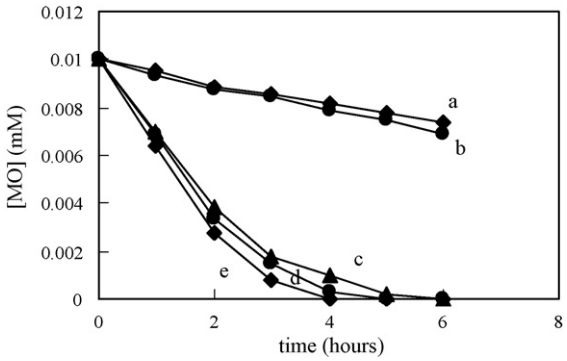

Fig. 3. Effect of H_2O_2 concentration on the discoloration of Methyl Orange (0.01 mM) at pH 5.9 under solar simulated light (90 mW/cm^2). (a) In the presence of H_2O_2 (0.7 mM), (b) in the presence of H_2O_2 (1.0 mM), (c) in the presence of TiO_2/Tedlar but no H_2O_2 added, (d) in the presence of TiO_2/Tedlar and H_2O_2 (0.7 mM) and (e) in the presence of TiO_2/Tedlar and H_2O_2 (1.0 mM).

TiO_2/Tedlar film on the discoloration rate is shown in Fig. 3, traces (d) and (e). This effect is seen to be much more important than the addition of small concentrations of H_2O_2 (Fig. 3, traces (a) and (b)). The presence of H_2O_2 and of the TiO_2/Tedlar further accelerates the Methyl Orange discoloration due to the electron acceptor role of H_2O_2

$$H_2O_2 + TiO_2(e^-) \rightarrow OH^- + OH^\bullet + TiO_2 \quad (7)$$

Fig. 4 traces (a) and (b) shows the discoloration of Methyl Orange under two different Suntest simulated solar light intensities. In the presence of TiO_2/Tedlar, the photo-discoloration is enhanced as seen in Fig. 4, traces (c) and (d) and this effect is more marked as the applied light intensity is increased from 60 to 90 mW/cm^2. That in Fig. 4a higher light intensity leads to a higher dye degradation kinetics implies that the saturation of Methyl Orange photosensitizer is not reached within the applied range of intensities.

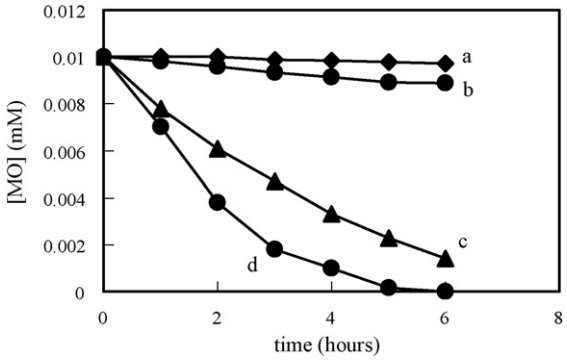

Fig. 4. Effect of the light intensity on the discoloration of Methyl Orange (0.01 mM) at an initial pH of 5.9. (a) Photolysis of the solution under solar simulated light (60 mW/cm^2), (b) photolysis of the solution under solar simulated light (90 mW/cm^2), (c) photolysis of the solution under solar simulated light (60 mW/cm^2) in the presence of TiO_2/Tedlar photocatalyst and (d) photolysis of the solution under solar simulated light (90 mW/cm^2) in the presence of TiO_2/Tedlar.

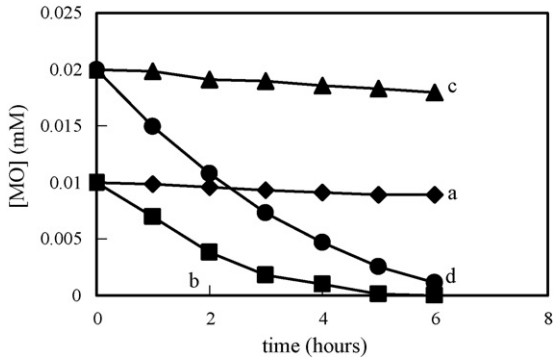

Fig. 5. Effect of the initial concentration of Methyl Orange on the discoloration rate under solar simulated light (90 mW/cm^2) at an initial pH of 5.9. (a) Dye solution 0.01 mM, (b) dye solution 0.01 mM in the presence of TiO_2/Tedlar photocatalyst, (c) dye solution 0.02 mM and (d) dye solution 0.02 mM in the presence of TiO_2/Tedlar.

3.3. Effect of the dye concentration on the discoloration kinetics. Stability of the TiO_2/Tedlar film

Fig. 5 shows the photo-discoloration of Methyl Orange in the absence (traces (a) and (c)) and in the presence of TiO_2/Tedlar catalyst as shown in traces (b) and (d). Fig. 5, trace (b) shows a half-life of about 2 h for the 0.01 mM dye solution and trace (d) shows a half-life of 2.5 h for the 0.02 mM dye concentration. The discoloration for a solution of Methyl Orange (0.02 mM) is therefore slower than for a solution of the same dye (0.01 mM), showing an inhibitory effect of the initial dye concentration on the rate of the photocatalyzed degradation.

Fig. 6 shows the true catalytic nature of the Methyl Orange discoloration. The first four cycles are shown for the abatement of this dye. The catalyst was washed after each cycle and then the dye was added in solution to carry out a new discoloration cycle. The degradation rate remained stable up to 3 months. The mechanical stability of the catalyst was found adequate for the reactor application.

3.4. Transmission electron microscopy of TiO_2/Tedlar films (TEM)

Fig. 7 shows the TiO_2 deposited on the rougher side of Tedlar (side 1). Fig. 8 shows the electron micrographs of TiO_2/Tedlar

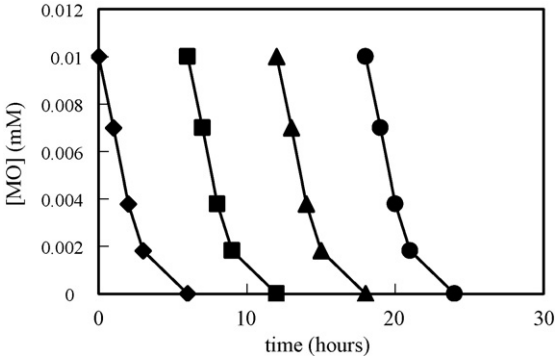

Fig. 6. Repetitive catalytic photo-discoloration cycles of Methyl Orange (0.01 mM) under solar simulated light (90 mW/cm^2) in the presence of TiO_2/Tedlar at an initial pH of 5.9.

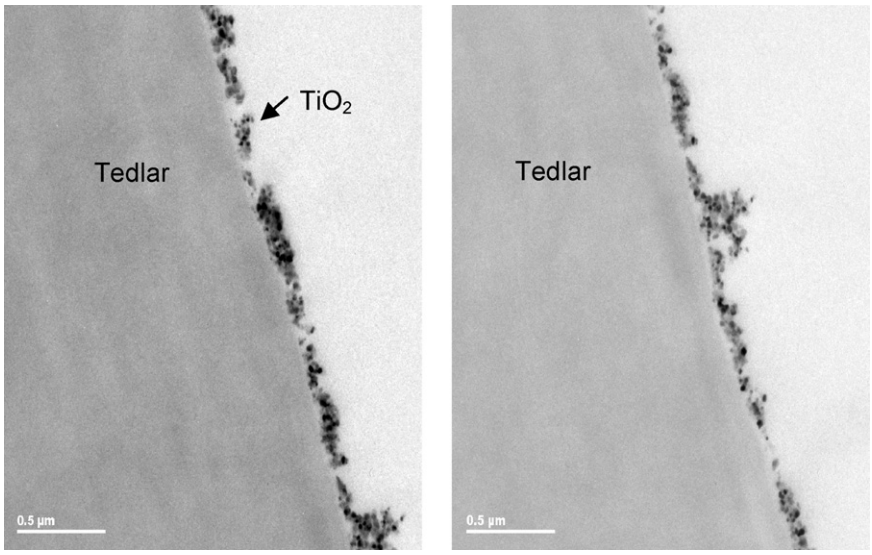

Fig. 7. Transmission electron microscopy of the TiO_2/Tedlar film photocatalyst before use in a photocatalytic reaction.

after 6 h Methyl Orange discoloration as performed in Fig. 2 trace (b). Fig. 7 shows that the Tedlar surface is not completely covered by TiO_2 and also shows the formation of discrete TiO_2 agglomerates. It is seen that the distribution of the TiO_2 after 6 h reaction (Fig. 8) is very close to the one observed in Fig. 7 at time zero. This explains the stable repetitive photocatalytic performance reported in Fig. 6.

3.5. Atomic force microscopy of TiO_2/Tedlar film (AFM)

Fig. 9 shows the AFM of Tedlar film within a projected surface of 2 μm by 2 μm. The lower dark section of the surface analyzed by AFM shows the distribution of the valleys of the Tedlar surface while the clear sections refer to the density of the peak heights of the Tedlar film. The cantilever used applies a force of 0.1 N/m and this is the applied force between the tip of the cantilever and the sample within a surface of 10–15 nm. The estimation of the root mean square roughness (rugosity in shorthand Rq) for Tedlar in Fig. 9 renders a value of 17.0 nm and the average roughness (Ra) was found to be 14.5 nm. Since Rq contains squared terms, large deviations from the average height are weighted more heavily than they are in the calculation of Ra. For the same reason, small deviations are given less weight in the calculation of Rq than Ra. The maximum peak height found by the addition of the peak height Rp 33.26 nm and Rv (low valley limiting value) of −32.50 nm adding up to 65.76 nm.

Fig. 10 shows the AFM of a TiO_2/Tedlar film after being used in the photo-discoloration of Methyl Orange under the experimental conditions shown in Fig. 2, trace (b). The values found for Rq (rms, mean square roughness) was 19.7 nm and of

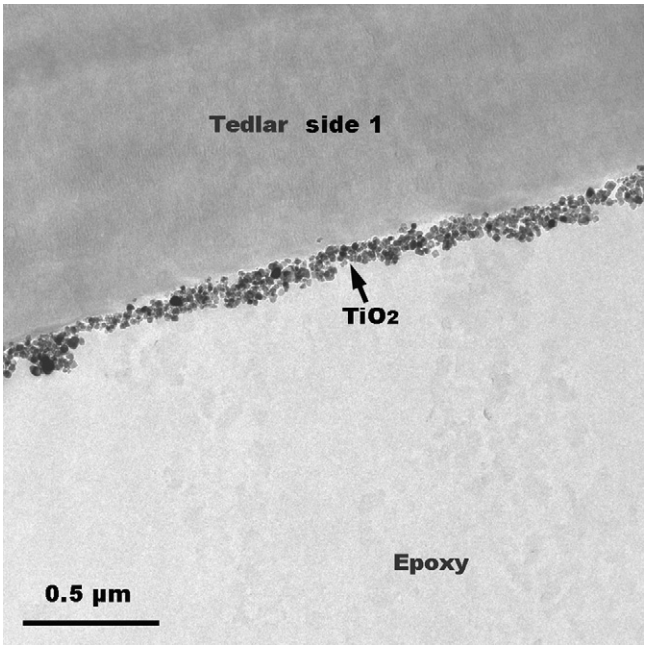

Fig. 8. Transmission electron microscopy of the TiO_2/Tedlar film photocatalyst after 6 h discoloration of Methyl Orange. For additional details see text.

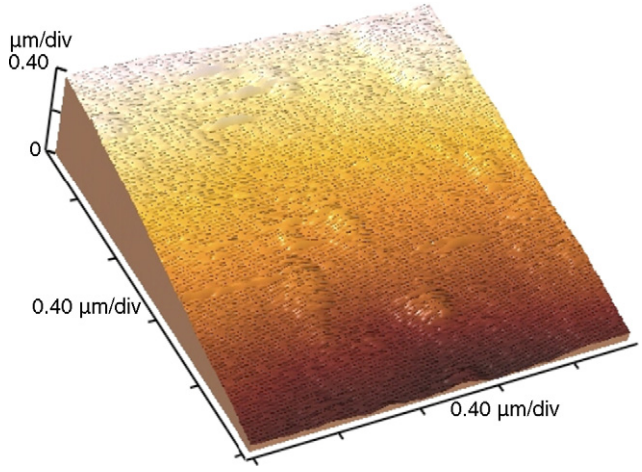

Fig. 9. Atomic force microscopy of Tedlar film.

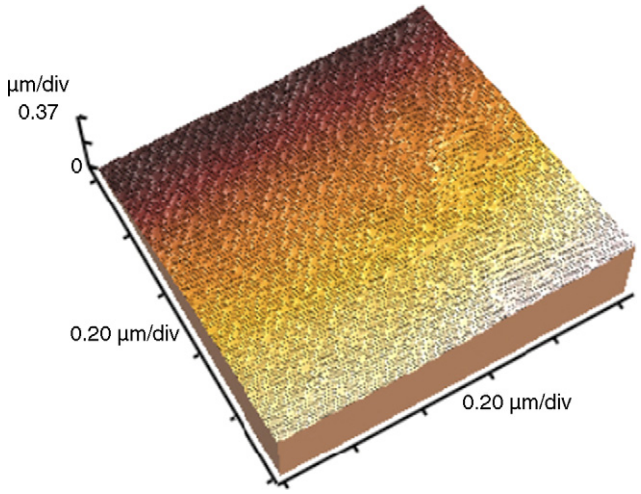

Fig. 10. Atomic force microscopy of the TiO_2/Tedlar film after Methyl Orange photo-discoloration.

Ra (average roughness) a value of 16.7 nm was found. The Rp (peak height) was of 44.6 nm and the Rv (low valley limiting value) was −29.6 nm. The two last values combined give a maximum peak height for the TiO_2 coating on the Tedlar film of 74.1 nm. The values of Rq and maximal height difference between the highest and the lowest surface point revealed little difference between the TiO_2/Tedlar films before and after Methyl Orange discoloration. This means that the surface of the sample is conserved during the discoloration process.

3.6. X-ray photoelectron spectroscopy (XPS) of TiO_2/Tedlar films

The XPS spectroscopy allows the determination surface composition of very thin outermost surface layer around 2 nm with very high surface sensitivity. The results obtained reveals significant changes taking place on the Tedlar at different reaction times in the TiO_2/Tedlar film during Methyl Orange discoloration. Tedlar as received showed the atomic surface concentration percentages for the following elements: Na(1.26%), F(12.26%), O(9.24%), N(0.91%), Ca(0.31%), C(75.66%) and S(0.27%). Elements like: Na, Ca, N, and S are present in the Tedlar surface structure. They are deposited during the film manufacture and were solely detected on the surface of Tedlar before any treatment. These elements were washed out during the TiO_2/Tedlar catalyst preparation. Tedlar film alone shows three major components: the two C 1s lines at 284.6 and 287.1 eV due to the presence of –CH and –CF groups, respectively and the F 1s line at 686.2 eV characteristic of the CF group. There is also the O 1s line at 531.7 eV indicating the presence of surface OH-groups. These groups are always present when TiO_2 is exposed to air.

Fig. 11 shows the XPS spectra of the C 1s in the topmost atomic layers. Fig. 11 trace (a) shows the $(–CH_2)_n$ peak at 284.5 eV and the $(–CHF–CH_2–)_n$ peak of Tedlar at 287.2 eV [15,16]. Trace (b) shows the attenuation of the $(CH_2)_n$ peak and the almost complete disappearance of the $(–CHF–CH_2–)_n$ peak when Tedlar is loaded with TiO_2. After one hour reaction,

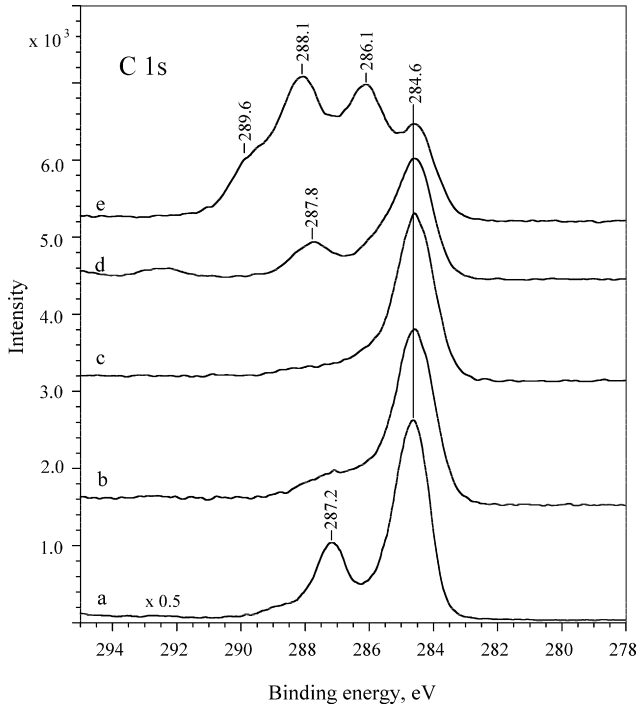

Fig. 11. C 1s signal for the Tedlar and TiO_2/Tedlar during the Methyl Orange photodiscoloration reaction. (a) Tedlar film alone, before reaction, (b) TiO_2/Tedlar film before reaction, (c) TiO_2/Tedlar film after 1 h reaction, (d) TiO_2/Tedlar film after 3 h reaction and (e) TiO_2/Tedlar film after 6 h reaction.

the lack of other peaks than C 1s at 284.6 eV indicates that (i) The TiO_2 is firmly attached to the Tedlar surface and (ii) the decomposition of Methyl Orange is a very fast surface reaction that proceeds without accumulation of intermediates (trace (c)). Fig. 11 trace (d) shows that after 3 h reaction the peak at 287.8 eV due to the presence of carboxyl groups. This suggests that the Tedlar aliphatic surface groups are oxidized to $–COO^-$ and that the TiO_2 surface particles interact with the Tedlar. The produced composite ensures a higher stability of the loaded TiO_2 particles on the Tedlar film. After 6 h of reaction with Methyl Orange the surface composition of the catalyst changes in a pronounced way. Fig. 11 trace (e) indicates the formation of surface groups having a lower content of hydrogen. There are three C 1s components at 286.1, 288.1 and 289.6 eV indicating surface oxidation species. The broad C 1s component at 288.1 eV suggests the presence of oxidation species such as carboxylic, carbonyl and –CF surface groups. The C 1s line at 286.1 eV indicates the formation of C–O surface groups. Finally, the low intensity component at 284.6 eV in Fig. 11e is due to the presence of surface CH– and $–CH_2$ groups.

Fig. 12, trace (a) shows the characteristic peak position of F 1s of vinylidene fluoride on the Tedlar fluorocarbon polymer $(–CHF–)_n$. The intensity of the F 1s peak at 686.3 eV in Fig. 12, trace (b) is attenuated after the TiO_2 is loaded on the Tedlar surface. This is an indication that TiO_2 particles are deposited on the F-containing groups of the Tedlar surface. The F 1s lines after one hour of reaction were observed at 683.7 eV (trace (c)) and 3 h at 683.6 eV (trace (d)) are characteristic of fluorine inorganic species. After 6 h, the surface fluorine undergoes

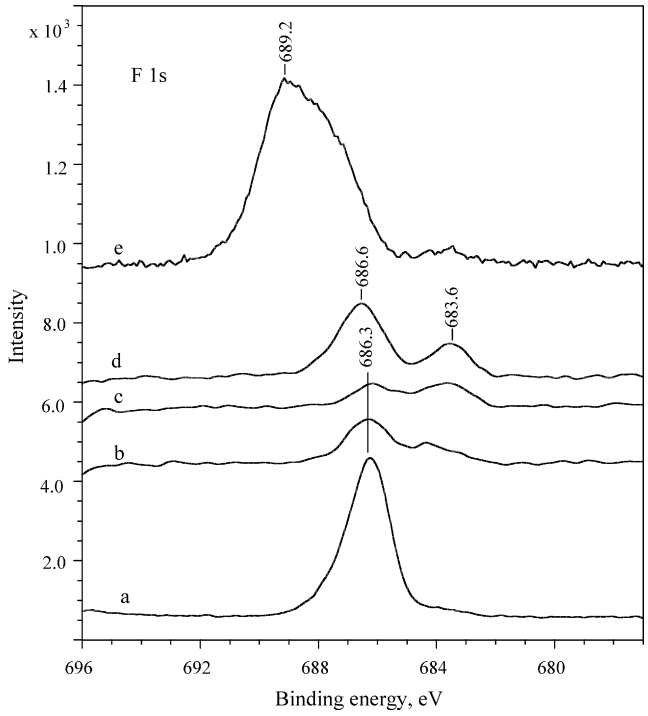

Fig. 12. F 1s signal for the Tedlar and TiO_2/Tedlar during Methyl Orange photodiscoloration reaction. (a) Tedlar film alone, before reaction, (b) TiO_2/Tedlar film before reaction, (c) TiO_2/Tedlar film after 1 h reaction, (d) TiO_2/Tedlar film after 3 h reaction and (e) TiO_2/Tedlar film after 6 h reaction.

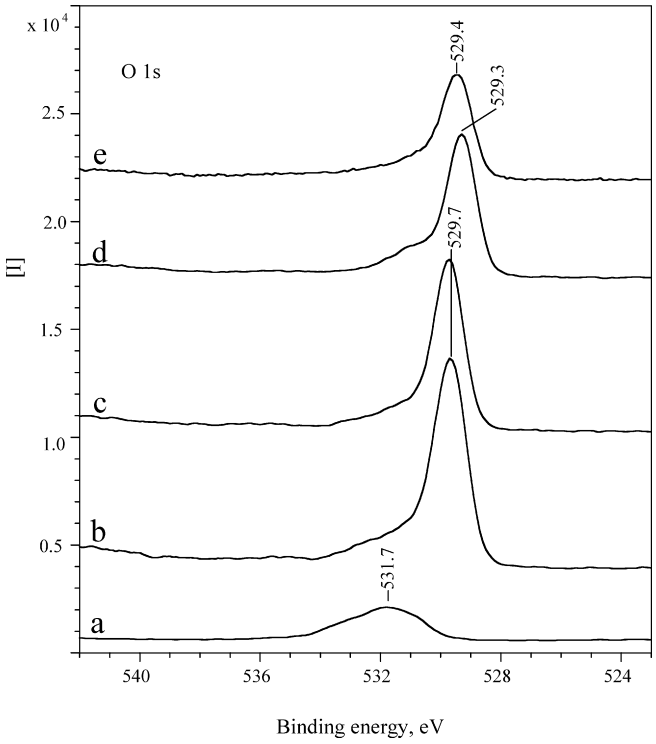

Fig. 13. O 1s signal for the Tedlar and TiO_2/Tedlar during Methyl Orange photodiscoloration reaction. (a) Tedlar film alone, before reaction, (b) TiO_2/Tedlar film before reaction, (c) TiO_2/Tedlar film after 1 h reaction, (d) TiO_2/Tedlar film after 3 h reaction and (e) TiO_2/Tedlar film after 6 h reaction.

significant changes. Fig. 12, trace (e) shows that the amount of surface fluorine increases significantly and their position shifts to a higher BE after this reaction time while the amount of surface carbon (Fig. 11) decreases. In fact this peak shows two components positioned at 689.1 and 688.5 eV suggesting some oxidation of the outermost layer of Tedlar at the end of the reaction.

Fig. 13, trace (a) shows the peak O 1s at 531.7 eV due to the H_2O_{ads} and OH_{surf} on the Tedlar film surface [1,2]. When the Tedlar was loaded with TiO_2 the O 1s was followed and trace (b) shows the shift of the O 1s line to 529.7 eV for the TiO_2/Tedlar catalyst before the discoloration reaction. This peak is due to the oxide-oxygen of TiO_2. The O 1s line (Fig. 13, trace (c) (d) (e)) shows a shift from 529.7 to 529.3 eV and then back to 529.4 eV after 6 h irradiation. This points to the regeneration and stability of the catalyst during the dye discoloration since this peak corresponds to the position of the TiO_2 peak. The TiO_2/Tedlar film before the discoloration reaction shows a strong signals for the TiO_2 doublet Ti $2p_{3/2}$ at 458.4 eV. But this Ti 2p line is shifted to lower BE by 0.3 eV after 3 h reaction indicating a partial reduction of TiO_2 and the presence on the catalyst surface of Ti(III) and Ti(IV) species. After 6 h reaction, when the Methyl Orange was completely decomposed, the oxidation state of TiO_2 shifted back to the position of the oxidation state at time zero. This means that the Ti(IV) oxidation state rebuilds again from its partially reduced TiO_2 form.

The photosensitization by Methyl Orange of the TiO_2/Tedlar leads to the formation of an azo-dye radical cation as documented in the literature [4,13,14]. On thermodynamic grounds the charge transfer has been reported to be possible

$$\begin{aligned}&\text{Methyl Orange} + \text{TiO}_2/\text{Tedlar} + h\nu\\ &\quad\rightarrow [\text{Methyl Orange}^* + \text{TiO}_2/\text{Tedlar}]\\ &\quad\rightarrow \text{Methyl Orange}^{\bullet+} + \text{TiO}_2e_{cb}-/\text{Tedlar}\end{aligned} \quad (8)$$

In Eq. (8) the initial oxidation state of Ti in TiO_2/Tedlar is (IV) and the dye photosensitization leads to the transient $TiO_2e_{cb}-$ or Ti(III). The TiO_2 participates in a redox type during the discoloration of Methyl Orange.

Finally, the highest intensity of the N 1s peak at 399.5 eV was found after 3 h reaction. After this the highest surface concentration of intermediates is found and this is in agreement with the largest concentration of Ti(III) detected by XPS. Calcium and nitrogen were not found any more after 6 h reaction.

3.7. Infrared spectroscopy of TiO_2/Tedlar films (ATRIR)

The recorded attenuated total reflection infrared spectroscopy (ATRIR) spectra of Tedlar alone and Tedlar loaded with TiO_2 after different reaction times are presented in Fig. 14. TiO_2 presents two strong absorbance bands at 360 and 573 cm^{-1} with a shoulder at 760 cm^{-1}, which appears in Fig. 14 in form of a strong increase of absorbance level below 800 cm^{-1}, in traces (b) through g). Above 900 cm^{-1}, the spectra of Tedlar loaded with TiO_2 are all similar to the Tedlar spectrum alone (Fig. 14, trace (a). There is no formation of additional absorbance bands due to intermediates on the catalyst surface. The only change after

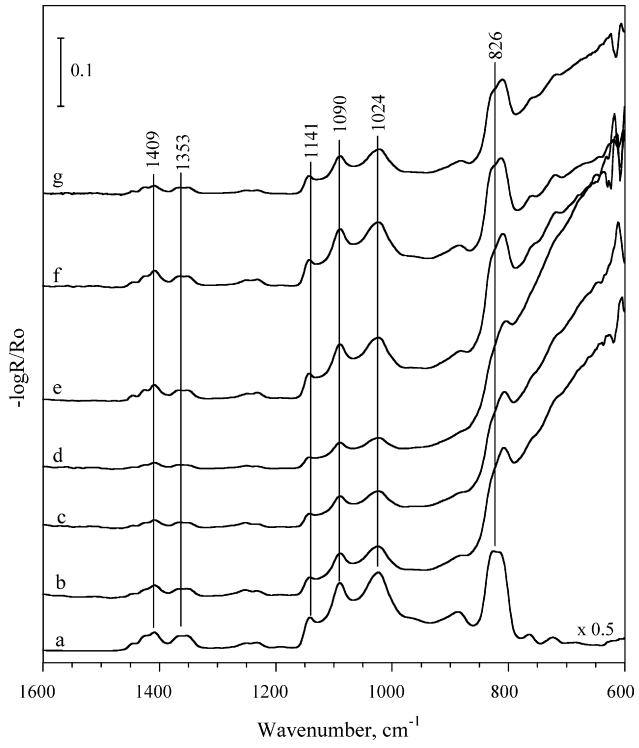

Fig. 14. Attenuated total reflection infrared spectroscopy (ATRIR) of Tedlar and TiO_2/Tedlar during Methyl Orange photodiscoloration reaction. (a) Tedlar film alone, before reaction, (b) TiO_2/Tedlar film before reaction, (c) TiO_2/Tedlar film after 1 h reaction, (d) TiO_2/Tedlar film after 3 h reaction, (e) TiO_2/Tedlar film after 4 h reaction, (f) TiO_2/Tedlar film after 5 h reaction and (g) TiO_2/Tedlar film after 6 h reaction.

the loading of TiO_2 on the Tedlar surface was the attenuated absorbance below 800 cm^{-1} due to the loss of some TiO_2 particle from the Tedlar as reported previously by TEM. Some bands are observed around 1400 cm^{-1} (Fig. 14) indicating the presence of surface CO_3^{2-} ions in agreement with the XPS observations reported in the preceding section.

3.8. Elemental analysis of TiO_2 of the Tedlar films (AAS)

The elemental analysis of the TiO_2/Tedlar films before catalytic runs showed a TiO_2 content of $0.88\% \pm 0.05\%$. For the same films after four consecutive dye photo-discoloration runs, the TiO_2 content was the same. The samples were analyzed by atomic absorption spectrometry using a Perkin-Elmer 300 s unit.

4. Conclusions

The synthesis and stabilization of a novel TiO_2-fluorocarbon composite photocatalyst is presented. This TiO_2-fluorocarbon composite can efficiently photocatalyze the discoloration of Methyl Orange, avoiding the separation of TiO_2 after the treatment. The treatment employed to fix TiO_2 on the C–F film introduced marked changes in the XPS spectra positions of C, O and F in the Tedlar film. Further changes in the position of the C, F and O during the photocatalysis were investigated by XPS. Evidence for the charge transfer between the semiconductor and the azo-dye is presented by XPS and ATRIR experimental data. ATRIR shows no formation of additional bands due to the intermediates produced by Methyl Orange degradation on the TiO_2/Tedlar confirming the efficiency of the photocatalytic process.

Acknowledgements

The financial support of COST 540 PHONASUM "Photocatalytic technologies and novel nano-surface materials, critical issues" is duly acknowledged.

References

[1] J. Winkler, Titanium Dioxide, Vincentz Network, Hannover, Germany, 2003.
[2] Th. Oppenlaender, Photochemical Purification of Water and Air, Wiley–VCH Verlag, Weinheim, 2003.
[3] J. Fernandez, J. Bandara, A. Lopez, Ph. Buffat, J. Kiwi, Langmuir 15 (1999) 185–192.
[4] M. Dhananjeyan, J. Mielczarski, K. Thampi, Ph. Buffat, M. Bensimon, A. Kulik, E. Mielczarski, J. Kiwi, J. Phys. Chem. B 105 (2001) 12046–12055.
[5] M. Fabiyi, L. Skelton, J. Photochem. Photobiol. A 132 (2000) 121–128.
[6] R. Naik, R. Joshi, R. Deshpande, J. Molec. Catal. A 238 (2000) 46–60.
[7] A. Matsuda, T. Matoda, T. Kogure, K. Tadanga, T. Minami, M. Tatsumisago, J. Sol–Gel Sci. Technol. 27 (2003) 61–69.
[8] M. Chan, T. Ko, H. Hiroaka, Surf. Sci. Rep. 24 (1999) 1–54.
[9] S. Al-Qaradawi, S. Salman, J. Photochem. Photobiol. A 148 (2002) 161–168.
[10] M. Stylidi, K. Kondarides, X. Verykios, Appl. Catal. B 47 (2004) 189–201.
[11] A. Shirley, Phys. Rev. B5 (1979) 4709–4918.
[12] Disperse Metal-oxides Degussa Brochure, 6342 Baar 2, Switzerland, 1997.
[13] K. Vinodgopal, P.V. Kamat, J. Photochem. Photobiol. A 83 (1994) 141–148.
[14] J. Bandara, J. Kiwi, New J. Chem. 23 (1999) 717–724.
[15] C. Wagner, W. Riggs, I. Davis, J. Moulder, G. Muilenberg (Eds.), Handbook of X-ray Photoelectron Spectroscopy, Perkin Elmer Corp., Eden Prairie, Minn., 55344. USA, 1989.
[16] D. Briggs, M. Shea, Practical Surface Analyisis, 2nd ed., John Wiley, Chichester, UK, 1990, v1.